Neurochemistry International 159 (2022) 105402

Contents lists available at ScienceDirect

Neurochemistry International

journal homepage: www.elsevier.com/locate/neuint

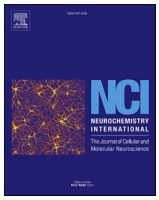

The role of NAD metabolism in neuronal differentiation

Diogo Neves [a,*], Brian J. Goodfellow [b], Sandra I. Vieira [a,1], Raquel M. Silva [a,c,1]

[a] Departamento de Ciências Médicas & Institute of Biomedicine (iBiMED), Universidade de Aveiro, Portugal
[b] Departamento de Química & CICECO, Universidade de Aveiro, Portugal
[c] Universidade Católica Portuguesa, Faculdade de Medicina Dentária, Centro de Investigação Interdisciplinar em Saúde, Viseu, Portugal

ARTICLE INFO

Keywords:
Neuronal differentiation
Neuritogenesis
NAD
NAPRT
QPRT
Neural regeneration

ABSTRACT

Background: Nicotinamide adenine dinucleotide (NAD) metabolism is involved in redox and non-redox reactions that regulate several processes including differentiation of cells of different origins. Here, the role of NAD metabolism in neuronal differentiation, which remains elusive so far, was investigated.

Material and methods: A protein-protein interaction network between neurotrophin signaling and NAD metabolic pathways was built. Expression of NAD biosynthetic enzymes in SH-SY5Y cells during retinoic acid (RA)/brain derived neurotrophic factor (BDNF) differentiation, was evaluated. The effects of NAD biosynthetic enzymes QPRT and NAPRT inhibition in neurite outgrowth, cell viability, NAD availability and histone deacetylase (HDAC) activity, were analyzed in RA- and BDNF-differentiated cells.

Results: Bioinformatics analysis revealed the interaction between NAD biosynthetic enzyme NMNAT1 and NTRK2, a receptor activated by RA/BDNF sequential treatment. Differences were found in the expression of NAD biosynthetic enzymes during neuronal differentiation, namely, increased QPRT gene expression along the course of RA/BDNF treatment and NAPRT protein expression after a 5-day treatment with RA. QPRT inhibition in BDNF-differentiated SH-SY5Y cells resulted in less neuritic length per cell, decreased expression of the neuronal marker β-III Tubulin and also decreased NAD^+ levels and HDAC activity. NAPRT inhibition had no effect in neuritic length per cell, NAD^+ levels and HDAC activity. Of note, NAD supplementation along with RA, but not with BDNF, resulted in considerable cell death.

Conclusions: Taken together, our results show the involvement of NAD metabolism in neuronal differentiation, specifically, the importance of QPRT-mediated NAD biosynthesis in BDNF-associated SH-SY5Y differentiation and suggest additional roles for NAPRT beyond NAD production in RA-differentiated cells.

1. Introduction

Neuronal differentiation involves several stages on its path toward becoming a mature neuron. The process includes the formation of the first neurites (neuritogenesis), axonal elongation and dendritic growth (neuronal polarization), and final maturation for proper synaptogenesis (Tojima et al., 2003). These events involve both intracellular signaling and extracellular cues that regulate the actin and microtubule networks, as well as secretory, endocytic and protein degradation pathways (Yap and Winckler, 2012). Understanding how neurons differentiate is of outmost relevance for e.g. neural regeneration and for the development of innovative therapies in this field.

Nicotinamide adenine dinucleotide (NAD) is a coenzyme involved in oxidation-reduction reactions for energy production, and is a substrate for NAD-consuming enzymes such as sirtuins (SIRTs), poly(ADP-ribose) polymerases (PARPs) and cADP-ribose synthases (Chiarugi et al., 2012; Imai and Guarente, 2014). NAD metabolism has a pivotal role in developing cells and tissues, mainly through the regulation of these enzymes. To keep adequate cellular NAD levels, NAD biosynthesis is supported by several routes: the *de novo* pathway from the amino acid tryptophan, and salvage pathways that comprise nicotinamide riboside (NR), nicotinamide (NAM) and nicotinic acid (NA) as initial precursors. In adult tissues, NAD synthesis from NAM is the preferred route, followed by NA in a subset of tissues including kidney, heart and gastrointestinal tract (Hara et al., 2007; Rajman et al., 2018). NAM and NA are converted to their respective mononucleotides by nicotinamide phosphoribosyltransferase (NAMPT) and nicotinate phosphoribosyltransferase (NAPRT), respectively, the rate-limiting enzymes in these pathways.

NAMPT is essential for myeloid and hematopoietic differentiation of

* Corresponding author. Institute of Biomedicine – iBiMED, University of Aveiro, Santiago Campus, 3810-193, Aveiro, Portugal.
E-mail address: datneves@ua.pt (D. Neves).
[1] Equally contributing authors.

https://doi.org/10.1016/j.neuint.2022.105402
Received 18 February 2022; Received in revised form 17 June 2022; Accepted 9 July 2022
Available online 16 July 2022

Abbreviations

AKT2	Isoform 2 of RAC-beta serine/threonine-protein kinase
BDNF	Brain-derived neurotrophic factor
C/EBPβ	CCAAT/enhancer-binding protein beta
DIV	Days in vitro
FBS	Fetal bovine serum
GAPDH	Glyceraldehyde-3-phosphate dehydrogenase
GAP-43	Growth associated protein-43
HDAC	Histone deacetylase
iPSCs	Induced pluripotent stem cells
NA	Nicotinic acid
NAAD	Nicotinic acid adenine dinucleotide;
NAD	Nicotinamide adenine dinucleotide;
NADSYN	Glutamine-dependent NAD synthetase
NAM	Nicotinamide;
NAMN	Nicotinic acid mononucleotide;
NAMPT	Nicotinamide phosphoribosyltransferase
NAPRT	Nicotinic acid phosphoribosyltransferase
NMDAR	N-methyl-D-aspartate receptor
NMN	Nicotinamide mononucleotide;
NMNAT	Nicotinamide mononucleotide adenyltransferase
NMRK	Nicotinamide riboside kinase
NR	Nicotinamide riboside;
NTRK2	Neurotrophic tyrosine kinase receptor type 2
PA	Phthalic acid
PARP	Poly(ADP-ribose) polymerase
PBS	Phosphate buffered saline;
PI	Propidium Iodide;
QPRT	Quinolinate phosphoribosyltransferase
QUIN	Quinolinic acid
RA	Retinoic acid
SIRT	Sirtuin
TRP	Tryptophan
2-HPCA	2-hydroxypyridine-3-carboxylic acid

human induced pluripotent stem cells (iPSCs) through the NAD-SIRT1 and NAD-SIRT2 pathways, respectively (Skokowa et al., 2009; Xu et al., 2021). Additionally, NAMPT ablation and consequent NAD insufficiency was shown to supress the ability of neural stem/progenitor cells (NSPCs) to differentiate into oligodendrocytes (Stein and Imai, 2014). Osteogenic differentiation from bone marrow-derived mesenchymal cells can also be regulated by NAMPT (He et al., 2017; Skokowa et al., 2009), and NAM can mediate retinal pigment epithelium differentiation (Meng et al., 2018). Adipogenic differentiation depends on the distribution of NAD concentrations between the nucleus and the cytoplasm. Decreased NAD availability and consequent decreased PARP1 activity in the nucleus enable the activation of the CCAAT/enhancer-binding protein beta (C/EBP$_\beta$), a key transcription factor involved in the early phase of adipogenic differentiation. In turn, increased cytoplasmic NAD enhances glucose metabolism in the cytoplasm. Both events are critical for adipocyte differentiation (Ryu et al., 2018). Despite these evidence in several niches, little is known about the role of NAD metabolism in neuronal differentiation.

The SH-SY5Y cell line is frequently used to study neuronal differentiation in vitro. Despite its heterogeneous nature, combining mostly immature neuronal cells (N-type) but also non-neuronal cells (S-type), the high capacity of the N-type cells to transdifferentiate make this cell line an optimal model to recapitulate *in vivo* development (da Rocha et al., 2021, 2015). Several growth conditions have been reported to induce a neuronal-like phenotype in these cells, being the combination of all-trans retinoic acid (RA) and brain-derived neurotrophic factor (BDNF) by far the most applied (Şahin et al., 2021). During differentiation, SH-SY5Y cells start to elongate and express a panel of neuronal markers that include β-III Tubulin and growth associated protein-43 (GAP-43) (Dwane et al., 2013).

In this study, we set out to explore the role of NAD metabolism in the SH-SY5Y neuronal differentiation model using RA-BDNF sequential treatment. The results suggest novel functions for NAPRT beyond NAD production and show that the *de novo* route through QPRT might be important to ensure proper NAD levels for neurons to differentiate.

2. Material and Methods

2.1. Bioinformatics analysis

Networks related to the neurotrophins signaling pathway were constructed based on protein-protein interactions reported in the literature and public data sources. First, the key proteins involved in the neurotrophins signaling pathway were retrieved from the KEGG PATHWAY database (https://www.genome.jp/kegg/pathway.html). All of these were sorted using the respective UniProt code and submitted to IntAct in October 2020 to generate the interactome for each protein, which was downloaded for further analysis.

A network map was then subsequently generated for each protein interactome using Cytoscape version 3.7.2 (Shannon et al., 2003). Non-human proteins were eliminated and protein interactomes were merged to create a global protein interactome. Furthermore, a final network was built by merging the hubs that directly interact with NAD biosynthetic enzymes.

2.2. SH-SY5Y neuroblastoma cell culture

Human neuroblastoma SH-SY5Y cells (ATCC) were grown in Minimal Essential Medium (MEM) supplemented with F-12, 10% FBS, 0.5 mM L-glutamine, 100 U/mL penicillin and 100 mg/mL streptomycin (Gibco, Invitrogen) at 37 °C/5% CO_2. These cells were enriched in neuroblastic N-type cells based on their lower adherence to cell plates than the S-type cells counterpart. After reaching 90% confluence, cells were subcultured and differentiated for 5 days with 10 μM retinoic acid (RA, Sigma-Aldrich) in 1% FBS medium (timepoint 5 days in vitro, DIV), and for further 2 or 4 days with 10 ng/mL of brain-derived neurotropic factor (BDNF, Sigma-Aldrich) in serum-free medium (timepoints 7 DIV and 9 DIV, respectively). For the inhibition of NAPRT enzymatic activity, cells were exposed to 1 mM 2-hydroxypyridine-3-carboxylic acid (2-HPCA, Sigma-Aldrich) 48 h before timepoint 5 DIV. 2-HPCA inhibits NAPRT in a dose-dependent manner (Piacente et al., 2017). For the inhibition of QPRT enzymatic activity, cells were exposed to 1 mM Phthalic acid (PA, Sigma-Aldrich) 48 h before timepoints 5 and 7 DIV. PA is specific for QPRT inhibition, including in neurons (Braidy et al., 2011). Non-differentiated cells grown in the same conditions, and cells RA- and BDNF-differentiated but not exposed to drug inhibitors, were used as controls.

2.3. Protein extraction and immunoblotting

Proteins were extracted from SH-SY5Y cells at timepoints 5, 7 and 9 DIV in RIPA lysis buffer (150 mM NaCl, 1% NP40, 0.5% sodium deoxycholate, 0.1% SDS, 50 mM Tris pH 8.0) with protease inhibitors (Roche) under mechanical harvesting using scrappers, followed by total protein quantification using the Pierce™ BCA Protein Assay Kit (Thermo). Protein samples (12 μg of total protein per lane) were separated in reducing SDS-PAGE gels, transferred to 0.45 μm nitrocellulose membranes (GE Healthcare Life Sciences) and blocked with 5% low fat

milk in TBS- 0.5% Tween. The following primary antibodies were used for immunoblotting: NAMPT (HPA047776, Sigma-Aldrich, 1:2000 dilution), NAPRT (HPA024017, Sigma Aldrich, 1:2000 dilution), β-III Tubulin (T8578, Sigma-Aldrich, 1:10000 dilution), Acetyl-p53 (Lys382, 710294, Invitrogen, 1:750 dilution), GAP-43 (ab5220, Abcam, 1:2000 dilution) and GAPDH (ab8245, Abcam, 1:2000 dilution). Depending on the primary antibody, anti-rabbit (7074S, Cell Signaling) or anti-mouse (7076S, Cell Signaling) IgG HRP-linked secondary antibodies were used, both in 1:5000 dilution. The Amersham ECL Prime Western Blotting Detection Reagent (GE Healthcare Life Sciences) was used as developing reagent and images were acquired using Chemidoc (Bio-Rad). Image Lab software (Bio-Rad) was used for densitometric analysis of protein immunoreactive bands.

2.4. RNA extraction, cDNA synthesis and RT-PCR

For gene expression experiments, cells were lysed at room temperature with TRIZOL and immediately stored at −80 °C or processed. RNA isolation and purification were conducted with Direct-zol™ RNA MiniPrep (Zymo Research) and the purity and quantity of the RNA was determined using a Nanodrop. Up to 1 μg of purified RNA was reversed transcribed using SensiFast cDNA synthesis kit (Meridian Bioscience). Gene expression of *NAMPT*, *NAPRT*, *QPRT*, *NADSYN* and *GAPDH* was assessed by Reverse Transcription Polymerase Chain Reaction (RT-PCR) using the QIAGEN Multiplex PCR kit (QIAGEN). The samples were amplified in a MyCycler™ thermocycler (BioRad). The RT-PCR conditions are described in Supplementary Table 1. The RT-PCR end products were resolved by 1.5% agarose gel electrophoresis and changes in gene expression were evaluated using the Gel Doc XR+ (Bio-Rad).

2.5. Cell viability assay

Cell viability was evaluated using flow cytometry analysis of Propidium Iodide (PI) stained cells. Cells were collected at different timepoints and washed twice with PBS. After its dissociation from plates with 0.05% trypsin-EDTA, the cellular suspension was centrifuged at 1000 rpm for 3 min. Further, the cell pellets were then resuspended in PBS and 5 μL of 1 mg/mL PI staining solution (BD Pharmingen™) was added in the dark. Proper negative and positive controls were analyzed in parallel. For the negative control (to remove background), cells were incubated without PI. For the positive control, cells were treated with 100 μM of hydrogen peroxide (H_2O_2). Cell death analysis was performed in the FL-2 region using a BD Accuri™ C6 Cytometer and the data was acquired and analyzed using BD Accuri™ C6 Software (BD Biosciences). Before plot acquisition, the cell suspension was filtered with a 40 μm cell strainer.

2.6. NAD quantification assay

Intracellular NAD^+ and NADH levels were measured using the NAD/NADH Kit (ab65348, Abcam) according to the manufacturer's instructions. Briefly, following differentiation, cells were counted and the same number of cells in each condition was incubated with the NAD/NADH extraction buffer. The extracted samples were then filtered through a 10 kDa spin column to remove enzymes that consume NADH rapidly. To detect NADH only, samples were heated at 60 °C for 30 min. This step was omitted for the detection of total NAD (NAD^+ + NADH). NAD^+ was converted to NADH by adding NADH developer, and final sample concentrations were obtained from a standard curve derived from a solution of known NADH concentration. The exact concentration of NADH and total NAD allowed for the quantification of NAD^+ by subtracting NADH from total NAD, and also to determine the NAD^+/NADH ratio [(Total NAD – NADH)/NADH)].

2.7. HDAC quantification assay

To evaluate the histone deacetylase (HDAC) activity, proteins were extracted from SH-SY5Y cells using NP-40 lysis buffer (150 mM sodium chloride, 1% NP-40, 50 mM Tris pH 8.0) with protease inhibitors (Roche), under mechanical harvesting using scrappers. HDAC activity was examined in an 50 μg total protein aliquot of the cells lysate, using the fluorometric HDAC activity assay kit (BioVision), as described by the manufacturer. HDAC activity was expressed in relative fluorescence units (RFU)/μg protein.

2.8. Neuritic network quantification

Phase contrast (PhC) imaging of SH-SY5Y live cultures was performed under an Olympus IX-81 widefield epifluorescence inverted microscope, equipped with a LCPlanFl20x/0.40 objective and the AnalySIS software. Cells were seeded at an initial density of $1x10^5$ cells per 35 mm plate and live images acquired at days 5 and 7 of differentiation (exposure time around 350–400 ms/image). Between 8 and 10 images were acquired per condition, with a total of about 1000 cells being analyzed, considering three independent experiments.

To extract the neuritic parameters, particularly the total neuritic length, the NeuronRead macro was used according to Dias et al. (2017). NeuronRead is a semi-automated ImageJ Macro able to extract relevant information from neuronal PhC and fluorescence images and a time and cost-effective morphometric tool (https://www.ua.pt/pt/ibimed/page/23714). The neuron body segmentation parameters were set by default (5 for median and morphological filter radius), while the threshold for cell body and neuritic recognition was adjusted manually. In general, threshold parameters were maintained constant in between conditions of the same experiment. The scale was defined considering the 20 × /0.4 objective used (3.1 pixels/μm). The final results were expressed as total neuritic length per cell, taking into account the number of cells evaluated in each image.

2.9. Statistical analysis

Data was expressed as mean ± SEM (standard error of the mean) of at least three independent experiments. Statistical analysis was conducted by one-way ANOVA followed by the Tukey test, or by the student t-test, using the GraphPad Prism® software. As indicated in each experiment, three levels of significance were used, taking in consideration the *p*-value.

3. Results

3.1. NAD biosynthetic enzymes interact with neuronal differentiation proteins

Neuronal differentiation activates several events involved in cells commitment, survival and cytoskeleton remodeling. One of these is called 'the neurotrophin signaling pathway' that, in the case of the SH-SY5Y cell model here used, is activated by RA-BDNF sequential treatment. In these cells, RA stimulates the expression of the neurotrophic tyrosine kinase receptor type 2 (*NTRK2* gene; TrkB receptor protein), to which the neurotrophin BDNF binds to; further treatment with BDNF results in the development of longer neuritic processes. To start understanding the potential role of NAD metabolism in this mechanism, the proteins involved in neurotrophin(s) signaling pathway(s) and their respective protein interactors were retrieved. These data was used to build a protein-protein interaction network and search for NAD biosynthetic enzymes that could interact with these proteins (Fig. 1). We found that nicotinamide mononucleotide adenyltransferase (NMNAT1), an enzyme downstream all NAD biosynthetic pathways, may participate in neuronal differentiation by interacting with the NTRK2/TrkB receptor, which is positively modulated by RA in SH-SY5Y cells (Guo et al.,

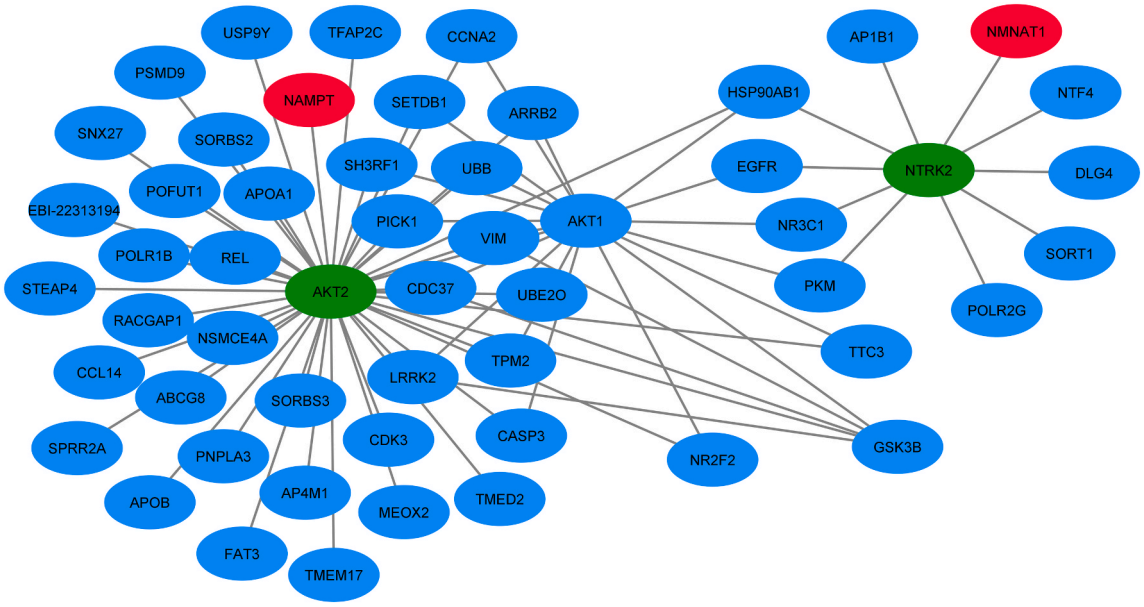

Fig. 1. Protein-protein interaction network showing the potential involvement of enzymes of NAD metabolism in the neurotrophin signaling pathway. This network was constructed using the Cytoscape software (version 3.7.2). Proteins involved in the neurotrophin(s) signaling pathway(s) were retrieved from the KEGG database and their respective protein-protein interactions were obtained using the IntAct database. Merged networks were obtained with Cytoscape. AKT2 and NTRK2 (green) are associated with neuronal differentiation and interact with NAD metabolism enzymes NAMPT and NMNAT1 (red), respectively.

2020). Furthermore, we also observed the interaction between NAMPT and AKT2, a protein that participates in the regulation of neuronal differentiation (Diez et al., 2012; Vojtek et al., 2003). These results suggest that enzymes involved in NAD biosynthesis are involved in neuronal differentiation pathways.

3.2. Expression of NAD biosynthetic enzymes is altered during SH-SY5Y cells differentiation

To induce neuronal differentiation, SH-SY5Y cells were sequentially treated with RA and BDNF for a total of seven days. SH-SY5Y cells continuously exposed to RA followed by treatment with BDNF, acquire morphological features of differentiation including elongation of the cell, extension of neuritic processes and their elongation (neurite outgrowth) (Fig. 2A, left panel, white arrows). Using NeuronRead, a semi-automated macro (Dias et al., 2017), we extracted morphometric data from our PhC microphotographs, particularly the total neuritic length per cell, whose increase after RA and RA-BDNF treatment corroborates continuous neuritogenesis (Fig. 2A, right graph). SH-SY5Y cells undergoing neuronal differentiation also displayed a sequential increase in the expression of the neuronal differentiation marker GAP-43, a protein enriched in neuritic growth cones, and β-III Tubulin, a neuronal-specific tubulin subtype and major constituent of neuronal microtubules (Encinas et al., 2000). RA-induced differentiation significantly increased the protein expression of GAP-43 at 5 DIV (Fig. 2B, left panel). On the other hand, β-III Tubulin protein expression increased after BDNF treatment (Fig. 2B, right panel, 7 DIV). These results validate our SH-SY5Y cells neuronal differentiation model, in accordance with previous work using similar approaches (Encinas et al., 2000; Guo et al., 2020).

Alterations in the levels of NAD biosynthetic enzymes during SH-SY5Y differentiation were further analyzed. A significant increase in the gene expression of quinolinate phosphoribosyltransferase (QPRT), an enzyme of the *de novo* route for NAD biosynthesis, was observed along the course of differentiation, and a significant decrease of *NAMPT* and *NAPRT* gene expression occurred after treatment with BDNF (day 7) (Fig. 2C). In addition, a significant increase in NAD Synthase (NADSYN) during neuronal differentiation was also detected. This enzyme belongs to the last step of two NAD biosynthetic pathways, which indicate that differentiating cells may depend on the *de novo* or NA routes for NAD production (Fig. 2D). Protein expression results also showed alterations in NAMPT and NAPRT enzymes. NAMPT had a significant decrease in protein expression during all the course of neuronal differentiation, while NAPRT had a significant increase during RA-induced differentiation followed by a return to its basal levels after the 2-day BDNF treatment (Fig. 2E). Overall, our data indicate changes in the expression of NAD metabolism enzymes during SH-SY5Y neuronal differentiation.

3.3. NAPRT inhibition does not affect the RA-induced differentiation phenotype and NAD availability

Considering that NAPRT protein levels increase at early RA-induced neuronal differentiation events, we further investigated the effect of its enzymatic activity inhibition in neuritogenesis, in NAD availability and in a NAD-dependent process. For this, we used 2-HPCA, a commercially available NAPRT inhibitor that prevents the conversion of NA to NAMN (Piacente et al., 2017). As mentioned above, in our cell model neuronal differentiation starts with RA-induced neuritogenesis. Total neuritic length per cell was quantified to understand the effect of NAPRT inhibition by 2-HPCA in that process. Our data demonstrates that 2-HPCA did not change the neuritic phenotype observed with RA (Fig. 3A).

To assess the effect of NAPRT inhibition in NAD metabolism, we further quantified NAD in undifferentiated and differentiated conditions with or without 2-HPCA. Our data showed a significant decrease in NAD^+ after RA-induced differentiation and no differences when 2-HPCA was applied to undifferentiated and differentiated cells. Moreover, the NAD^+/NADH ratio was not affected (Fig. 3B). In fact, the addition of 10 mM NAD to cells being differentiated with RA decreases their viability, as shown by the 20% increase in PI positive cells, an effect not observed in undifferentiated cells (Fig. 3C). Since NAD^+ levels decrease following differentiation with RA, we measured the HDAC (histone deacetylase) activity. Despite quantifying all the HDAC activity including NAD-independent enzymes, decreased NAD^+ levels lead to a decreased rate of deacetylation by negatively influencing type III HDACs (sirtuins). The results showed that the HDAC activity decreases during RA-induced differentiation, as reported in the literature, and NAPRT inhibition did

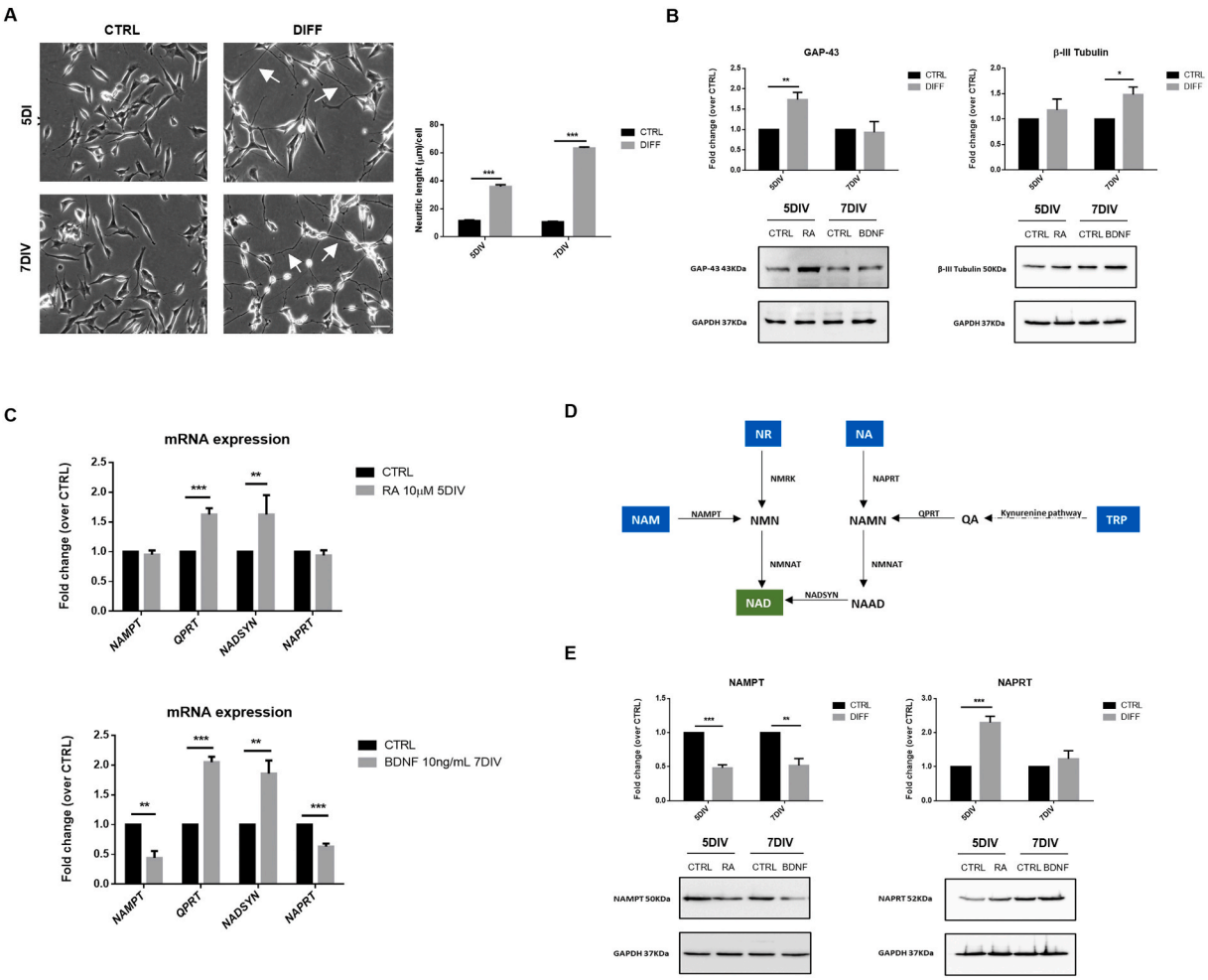

Fig. 2. RA-BDNF sequential treatment changes the expression of NAD biosynthetic enzymes during SH-SY5Y neuronal differentiation. A. Phase contrast representative images showed the continuous neurite outgrowth (arrows) during differentiation (left panel, scale bar: 50 µm) with the corresponding quantification of neuritic length per cell (right panel) B. Western blots demonstrated an increase in the expression of the differentiation marker GAP-43 at 5 days in vitro (DIV), and an increase in the expression of the differentiation marker β-III Tubulin following BDNF treatment at 7 DIV. C. RT-PCR results showed an increase of gene expression levels for *QPRT* and *NADSYN* on day 5 (upper panel, 5 DIV) and day 7 (lower panel, 7 DIV), and a decrease in *NAMPT* and *NAPRT* on day 7 (lower panel, 7 DIV). *GAPDH* was used as an internal control. D. Schematic representation of the NAD biosynthesis pathway with the main precursors for NAD production in mammalian cells (in blue) and respective intermediates E. Western blots showed decreased protein levels of NAMPT during all the time course of differentiation and increased protein levels of NAPRT at the end of the RA treatment (5 DIV). GAPDH was used as internal control. NAM, nicotinamide; NA, nicotinic acid; TRP, tryptophan; NR, nicotinamide riboside; NMN, nicotinamide mononucleotide; NAMN, nicotinic acid mononucleotide; NAD, nicotinamide adenine dinucleotide; NAAD, nicotinic acid adenine dinucleotide; NAMPT: nicotinamide phosphoribosyltransferase; NAPRT, nicotinic acid phosphoribosyltransferase; NMRK, nicotinamide riboside kinase; QPRT, quinolinate phosphoribosyltransferase; NMNAT, nicotinamide mononucleotide adenyltransferase; NADSYN, glutamine-dependent NAD synthetase. *, $p < 0,05$; **, $p < 0,01$; ***, $p < 0,001$.

not affect this rate (Fig. 3D). Taken together, our results suggest additional function for NAPRT beyond NAD^+ production and imply that a decrease in NAD^+ levels is mandatory for RA-induced SH-SY5Y differentiation.

3.4. QPRT inhibition affects the BDNF-induced differentiation phenotype and NAD availability

Along the neuronal differentiation time-course an increase in *QPRT* gene expression was observed. To elucidate this, the inhibition of QPRT enzymatic activity was performed using phthalic acid (PA), a commercially available QPRT inhibitor that prevents the conversion of QA into NAMN. The addition of PA to SH-SY5Y cultures during the RA differentiation had no effect on neurite outgrowth (Fig. 4A, right panel). However, PA had an effect in the subsequent BDNF-induced neuritic elongation, by reducing the average total neuritic length per cell from 60 to 40 µm. This corresponds approximately to a 30% decrease in neuritic elongation (Fig. 4B, right panel). The observed phenotype is reflected on the expression of β-III Tubulin, since the addition of PA led to a consistent decrease in the levels of that neuritic-associated neuronal marker (Fig. 4C). To evaluate the effect of PA-induced QPRT inhibition on NAD availability, NAD quantification was assessed. No differences were found when PA was applied to both undifferentiated and differentiated cells (Fig. 4D). However, following BDNF-induced differentiation, a significant increase in NAD^+ levels and in the NAD^+/NADH ratio were found, an effect that was reverted when PA and BDNF were combined (Fig. 4E). In line with this, when NAD was applied along with BDNF in cell cultures at later stages of neuronal differentiation no cell death was observed (Fig. 4F), unlike for RA-mediated earlier differentiation stages. In addition, the HDAC activity was measured and a decrease was observed at 7 DIV in BDNF-differentiating cells (Fig. 4G). Contrary to RA-induced differentiation where PA had no effect (Sup. Fig. 1), a further decrease in HDAC activity occurred when PA and BDNF were combined (Fig. 4G). This evidence is in accordance with NAD^+

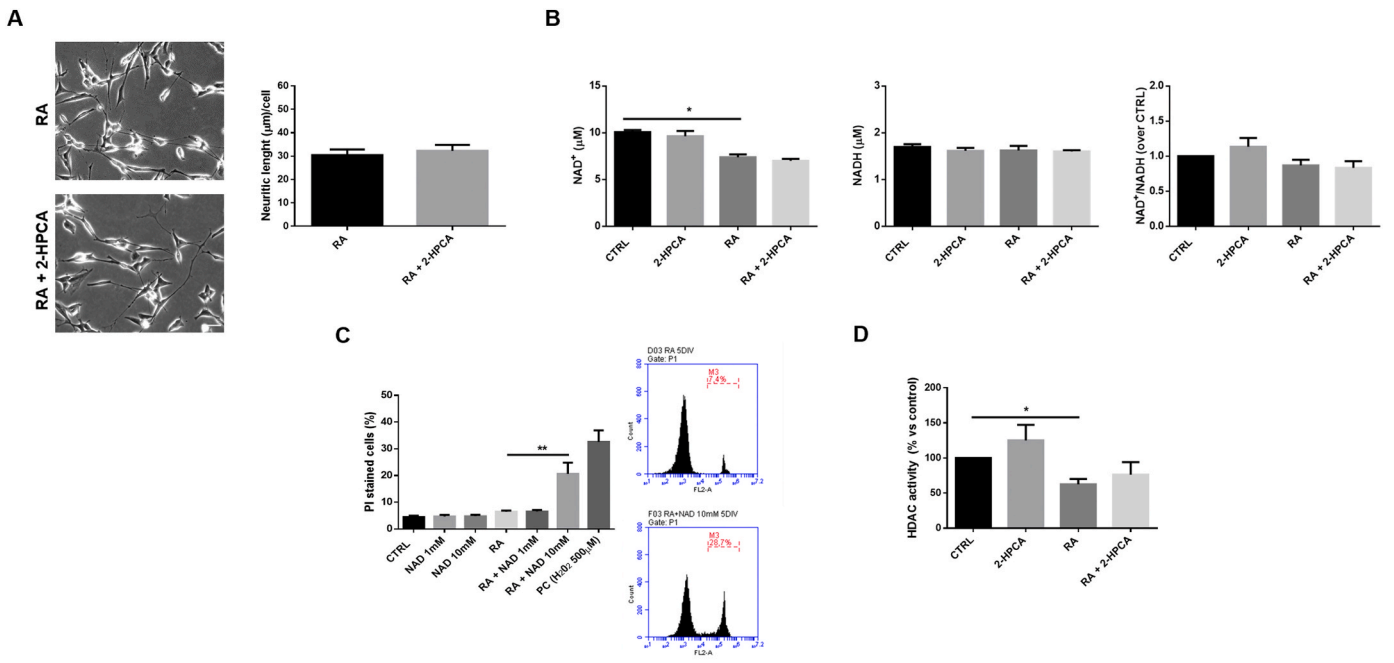

Fig. 3. Inhibition of NAPRT enzymatic activity does not affect RA-induced SH-SY5Y differentiation. A. Representative PhC microphotographs of live SH-SY5Y cells differentiated with 10 μM RA for 5 days in vitro (DIV) exposed or not to 1 mM 2-HPCA in the last 48h to inhibit NAPRT activity (scale bar: 50 μm). The neuritic length per cell upon RA-induced differentiation, in the presence or absence of 2-HPCA, was quantified and showed no significant alterations. B. SH-SY5Y cells differentiated or not with 10 μM RA for 5 DIV were exposed or not to 1 mM 2-HPCA in the last 48h. NAD quantification revealed a significant decrease in NAD^+ content following RA-induced differentiation and no differences were found when 2-HPCA was applied to both undifferentiated and differentiated cells. NAD^+/NADH ratio also showed no significative alterations between conditions. C. PI staining assay and flow cytometry plots indicated that contrarily to undifferentiated cells, 10 mM NAD induced an increase in the percentage of PI positive cells in RA-induced SH-SY5Y differentiated cells. Positive control (PC) was performed using hydrogen peroxide, H_2O_2. For statistical analysis, the effect of NAD supplementation was compared separately to CTRL or RA 10 μM 5DIV (undifferentiated and differentiated cells, respectively). D. SH-SY5Y cells differentiated or not with 10 μM RA for 5 DIV were exposed or not to 1 mM 2-HPCA in the last 48h to inhibit NAPRT activity. RA induced a significant decrease in the rate of histone deacetylation, but no further alterations occurred when RA and 2-HPCA were combined. *, $p < 0,05$; **, $p < 0,01$.

levels quantified and strongly indicates that QPRT-mediated NAD^+ synthesis is needed for proper BDNF-induced SH-SY5Y differentiation. This represents a distinct metabolic phase where NAD is needed. Altogether, these results show that the *de novo* route for NAD synthesis is important for BDNF-induced later stages of neuronal differentiation.

4. Discussion

Understanding neuronal differentiation has been challenging over the years, but of outmost importance for basic and applied research, including for developing neuronal regeneration strategies. Most neuronal differentiation studies include human iPSCs, embryonic stem cells (ESC) and cell lines capable of being transdifferentiated in culture, such as PC-12 and SH-SY5Y (Chuang et al., 2015; Sierra-Fonseca et al., 2014; Varderidou-Minasian et al., 2020; Zhang et al., 2021). In the cell model here used, the sequential treatment of SH-SY5Y cells with morphogens like RA and the neurotrophin BDNF induces a switch off in cellular proliferation and deep transcriptomic and structural changes towards neuronal differentiation (da Rocha et al., 2015; Dias et al., 2017; Encinas et al., 2000).

NAD and NAD-related biosynthetic enzymes have been reported to participate in cell differentiation processes of various types of cells and tissues, including muscle, adipose, blood, bone and neural tissues (in this later in glial cells) (Fletcher et al., 2017; He et al., 2017; Imai and Guarente, 2014; Ryu et al., 2018; Skokowa et al., 2009). As such, here we investigated whether NAD metabolism is also involved in the neuronal differentiation process and found alterations in the expression of the NAD metabolism enzymes NAMPT, NAPRT, QPRT and NADSYN in different neuronal differentiation conditions. Protein expression results revealed diminished expression levels for NAMPT, the rate limiting enzyme of the NAM route, throughout the SH-SY5Y neuronal differentiation time course. NAMPT overexpression is related to cell proliferation, particularly in tumoral microenvironments where high energetic demands are required. Neurons are non-proliferative cells, and SH-SY5Y cells undergoing neuronal differentiation stop to proliferate, which can explain the concomitant lower NAMPT levels, and may be related to the NAMPT-NAD-SIRT1 axis. In fact, NAD levels decrease in our RA-differentiated SH-SY5Y cells model as seen in the differentiation of other cells, such as muscle cells (Fulco et al., 2003). This may be related to reduced sirtuin activity, as suggested by the decreased HDAC deacetylation observed throughout the neuronal differentiation process and the increase in the acetylation of p53 in the RA-differentiated condition (Sup. Fig. 2). P53 is a substrate of SIRT1 and its deacetylation is associated with proliferative environments such as cancer. Since early differentiating cells stop proliferation and their NAD levels decrease, SIRT1 activity may also decrease, resulting in an increase of the p53 acetylation status. The decrease in NAD levels and the nuclear localization of SIRT1 suggest that at least nuclear NAD levels drop during the early phase of differentiation, which can be related with the shutdown of the NMNAT1 enzyme. In our bioinformatic analysis, the association of NMNAT1 with NTRK2, the TrkB receptor of the neurotrophin BDNF, both involved in a common neuronal differentiation pathway activated by the RA-BDNF sequential treatment, further supports this.

These results are in line with previous data demonstrating that the degree of acetylation of transcription factors and histones in neurons is increased and stimulates neuronal differentiation (Gaub et al., 2010; Shukla and Tekwani, 2020). A recent paper emphasized that SIRT1 expression decreases after a 5-day treatment with RA (Fu et al., 2019),

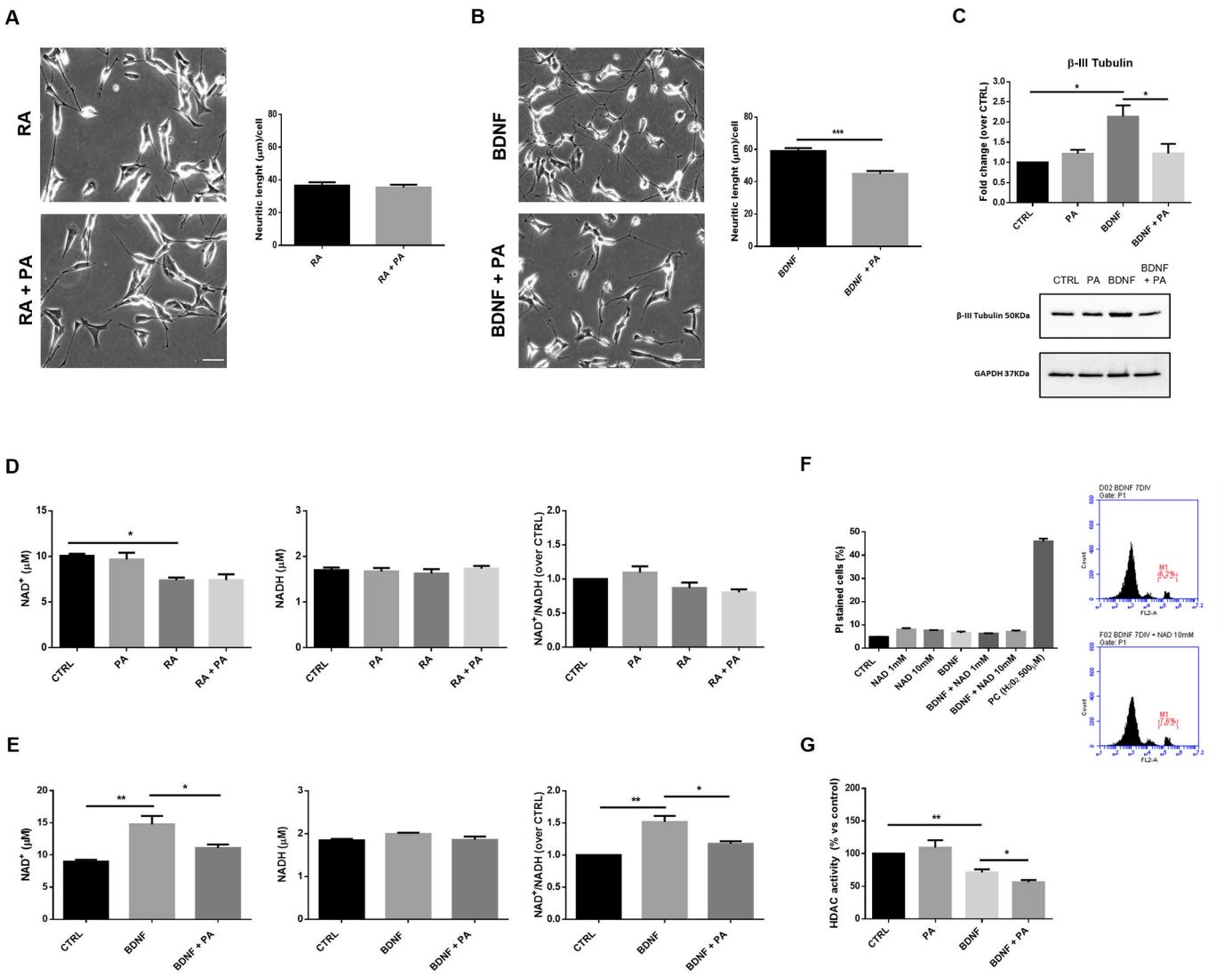

Fig. 4. Inhibition of QPRT enzymatic activity affects BDNF-induced SH-SY5Y differentiation. A. Representative PhC microphotographs of live SH-SY5Y cells differentiated with 10 µM RA for 5 days in vitro (DIV), exposed or not to 1 mM PA in the last 48h to inhibit QPRT activity (scale bar: 50 µm). Right graph: quantification of the neuritic length per cell during RA-induced differentiation with or without PA showed no alterations in the RA-induced differentiation phenotype following PA addition. B. Representative PhC microphotographs of live SH-SY5Y cells differentiated with10 µM RA for 5 days and 10 ng/ml BDNF for further 2 days, exposed or not to 1 mM PA in the last 48h (scale bar: 50 µm). Right graph: quantification of the neuritic length per cell during differentiation with or without PA showed alterations in the differentiation phenotype following PA addition. C. Western blots indicated that PA decreases the expression of β-III Tubulin after 2 days of BDNF-induced differentiation (7 DIV). D. SH-SY5Y cells differentiated or not with 10 µM RA for 5 DIV were exposed or not to 1 mM PA in the last 48h. NAD quantification revealed no differences when PA was applied to both undifferentiated and differentiated cells. NAD^+/NADH ratio also showed no significative alterations between conditions. E. SH-SY5Y cells differentiated or not with 10 µM RA for 5 DIV and 10 ng/mL BDNF for further 2 days and exposed or not to 1 mM PA in the last 48h. NAD quantification revealed a significant increase in NAD^+ content following BDNF-induced differentiation and this effect was reverted when PA was applied to differentiated cells. NAD^+/NADH ratio also showed significant alterations between conditions. F. PI staining assay and flow cytometry plots indicated that neither 1 mM nor 10 mM NAD affected cell viability in BDNF-induced SH-SY5Y differentiated cells. Positive control (PC) was performed using hydrogen peroxide, H_2O_2. For statistical analysis, the effect of NAD supplementation was compared separately to CTRL or BDNF 10 ng/mL 7DIV (undifferentiated and differentiated cells, respectively). G. SH-SY5Y cells differentiated or not with 10 µM RA for 5 days and 10 ng/ml BDNF for further 2 days were exposed or not to 1 mM PA in the last 48h. BDNF induced a significant decrease in the rate of histone deacetylation, and even a more pronounced decrease was found when BDNF and PA were combined. *, $p < 0,05$; **, $p < 0,01$; ***, $p < 0,001$.

while another stated that the SIRT1 inhibitor EX-527 accelerates RA-mediated neurogenesis in embryonic P19 cells (Kim et al., 2016). Other studies showed that SIRT1 can function as a co-repressor of the retinoic acid receptor (RAR) localized in the nucleus (Yu et al., 2012) and its deficiency was able to increase the acetylation status of cellular retinoic acid binding protein II (CRABPII), promoting differentiation of mouse ESC through RA signaling (Tang et al., 2014). It is also important to refer that, unlike the early phases of neuronal differentiation where SIRT1 inhibition seems to be important (as during the RA exposure stage in our cell model), there may be a timepoint in the process where this inhibition is no longer present, as SIRT1 deficiency retards axogenesis and dendritic branching in embryonic hippocampal neurons (Li et al., 2013; Tang et al., 2014). Our results with NAD supplementation also support this, as NAD addition to cultures under differentiation with RA (earlier stage) led to increased cell death, contrary to NAD addition to BDNF-treated cells (later neuronal differentiation stage). Recently, exposure to NAD was shown to inhibit morphological development of neural progenitor cells (NPCs) into neurons (Huang et al., 2022). SIRT1 activation has been related with a shift into the astroglial lineage in NPCs (Prozorovski et al., 2008), therefore, the initial decrease in NAD

levels may be related with decreased SIRT1 activation in order to promote the commitment of cells to become neurons.

Another NAD metabolic alteration was found for QPRT, a major enzyme of the *de novo* route for NAD biosynthesis, whose levels increase during the course of SH-SY5Y neuronal differentiation. QPRT catabolizes quinolinic acid (QUIN), which is also an agonist of N-methyl-D-aspartate receptors (NMDAR). QUIN accumulation in the brain functions as a neurotoxin causing energy disfunction, oxidative stress, inflammation, and cell death (Lugo-Huitrón et al., 2013). In SH-SY5Y cells and primary neuronal cultures, QUIN in low concentrations increases neuritic network, possibly via NAD production (Hernandez--Martinez et al., 2017; Huang et al., 1995). More recently, *Haslinger* et al. pointed to a neurodevelopmental protective role for QPRT in SH-SY5Y cells using knock out (KO) systems and enzymatic inhibition with phthalic acid (Haslinger et al., 2018). The authors found considerable cell death by inhibiting QPRT in RA/BDNF-induced SH-SY5Y differentiated cells, contrary to proliferative cells, where cell death was almost absent. Additionally, low NAD levels have been related to DNA hypermethylation at the BDNF promoter IV and decreased transcription (Chang et al., 2010). Our results indicated that QPRT function is important for BDNF-mediated SH-SY5Y differentiation as its inhibition with PA diminished the neuritic network as well as the expression of the neuronal marker β-III Tubulin. Considering the association between NAD and BDNF, we suggest that differentiated cells in our model exhibit less neurites with QPRT inhibition due to the lack of NAD synthesis through the *de novo* pathway. This is also reinforced by the NAD quantification and HDAC activity assays. NAD $^{+}$ quantification showed that NAD $^{+}$ levels increase following BDNF addition, an increase reverted by PA-induced QPRT inhibition. Contrary to the observed in the differentiation with RA, the NAD^{+}/NADH ratio is also affected in the differentiation with BDNF and QPRT inhibition. As the NAD^{+}/NADH ratio reflects the overall status of mitochondrial metabolism and differentiated cells require an increase in ATP levels, defects in the redox status are likely to happen when NAD^{+} is depleted. Additionally, less HDAC activity for cells treated with BDNF and PA was observed when compared to BDNF alone. As a matter of fact, at least the activity of type III NAD-dependent HDACs may be important for BDNF-mediated SH-SY5Y differentiation. SIRT1 regulates BDNF expression and has a role in the differentiation of neural precursor cells (Hisahara et al., 2008; Zocchi and Sassone-Corsi, 2012) and SIRT6 is highly expressed during neurite development in hippocampal neurons (Matsuno et al., 2021). The involvement of other sirtuins, such as SIRT3, in neuronal differentiation studies should be a matter of future investigations in this field. SIRT3 deacetylation has already been associated with an increase in pyruvate dehydrogenase activation and possibly mitochondrial oxidative phosphorylation, in cancer cells (Ozden et al., 2014).

We also found an increase in *NADSYN* expression over the time course of SH-SY5Y differentiation. NADSYN is involved in the last step of NAD biosynthesis from NA and the *de novo* routes, and our data show that *NADSYN* overexpression may be associated with the increase in QPRT expression in BDNF-induced differentiation. Although QPRT and NADSYN increased gene expression was also seen during RA-mediated differentiation, the cell death effect of increased NAD under this differentiation stage, and the absence of PA effects on the RA-differentiation phenotype, NAD levels and on HDAC activity, may exclude the *de novo* route as NAD production source during this earlier differentiation period.

Lastly, a significant increase in the NA rate limiting enzyme NAPRT was found following a 5-day RA treatment, with a significant decrease in the NAPRT gene and protein expression in the following 2-day and 4-day treatment with BDNF, respectively (Fig. 2D and Sup. Fig. 3). Despite lower NAPRT (and also NAMPT) expression in the adult brain when compared to other tissues (Duarte-Pereira et al., 2016), SH-SY5Y cells appear to require NAPRT in the neuronal differentiation process, at least in early stages. Inhibition of NAPRT enzymatic activity with 2-HPCA did not affect RA-induced SH-SY5Y neuronal differentiation, as shown by the absence of effects in neuritic network phenotype, NAD^{+} levels, NAD^{+}/NADH ratio and the rate of HDAC deacetylation. The increase in cell death seen when a high concentration of NAD was added to RA-differentiated cultures also suggests that NAPRT has a role beyond the production of NAD during RA-induced SH-SY5Y differentiation, as previously proposed (Duarte-Pereira et al., 2021).

NAPRT has been mostly studied in the context of NAD biosynthesis, especially in cancer (Duarte-Pereira et al., 2016; Galli et al., 2020). However, recent studies suggest novel functions for NAPRT that are independent of its enzymatic activity. One of these links NAPRT to canonical Wnt signaling, and the aggressiveness of epithelial to mesenchymal (EMT) subtype tumors (Lee et al., 2018). Another is related to inflammatory processes, where the extracellular form of NAPRT (eNAPRT) was found to enhance the differentiation of circulating monocytes into macrophages, and induce the activation of the inflammasome and the secretion of inflammatory cytokines (Managò et al., 2019). In another context, NA has been related with epidermal differentiation in damaged skin (Bermudez et al., 2011). Considering NAPRT downregulation following BDNF addition, we wonder whether NA-related signaling is needed somewhere at later differentiation stages.

5. Conclusions

Overall, our results first demonstrate the importance of the *de novo* NAD biosynthesis pathway for BDNF-mediated later neuronal differentiation stages, including neuritogenesis, and also suggest, for the first time, a novel role for NAPRT in earlier stages of neuronal differentiation. Future studies may address NAPRT expression in this context and also the concrete function(s) of NAPRT and QPRT in the neuritogenic process. In addition, exploring NAPRT as a key player involved in the differentiation of other types of cells and tissues may be investigated as well.

Ethics approval and consent to participate

Not applicable.

Funding

This work was supported by FCT (Fundação para a Ciência e Tecnologia), FEDER (Programa Operacional Factores de Competitividade – COMPETE) and by QREN, through the grant SFRH/BD/129409/2017 to DN, and the projects GoBack (PTDC/CVT-CVT/32261/2017), UIDB/04501/2020 (POCI-01-0145-FEDER-007628) to iBiMED, UIDB/04279/2020 to CIIS and UIDB/50011/2020 & UIDP/50011/2020 to CICECO. Image acquisition was performed in the LiM facility of iBiMED, a node of PPBI (Portuguese Platform of BioImaging): POCI-01-0145-FEDER-022122. FCT/MCTES and UCP support CEEC institutional funding of RMS (CEECINST/00137/2018/CP1520/CT0012).

Author contributions

DN and RMS designed the study. DN performed the experiments and drafted the manuscript. All authors read and approved the final manuscript.

Consent for publication

Not applicable.

Data availability statement

All data generated or analyzed during this study are available from the corresponding author on reasonable request.

Declaration of competing interest

The authors declare no competing interests.

Appendix A. Supplementary data

Supplementary data to this article can be found online at https://doi.org/10.1016/j.neuint.2022.105402.

References

Bermudez, Y., Benavente, C.A., Meyer, R.G., Coyle, W.R., Jacobson, M.K., Jacobson, E.L., 2011. Nicotinic acid receptor abnormalities in human skin cancer: implications for a role in epidermal differentiation. PLoS One 6, e20487.

Braidy, N., Guillemin, G.J., Grant, R., 2011. Effects of kynurenine pathway inhibition on NAD metabolism and cell viability in human primary astrocytes and neurons. Int. J. Tryptophan Res. 4, 29–37. https://doi.org/10.4137/IJTR.S7052.

Chang, J., Zhang, B., Heath, H., Galjart, N., Wang, X., Milbrandt, J., 2010. Nicotinamide adenine dinucleotide (NAD)-regulated DNA methylation alters CCCTC-binding factor (CTCF)/cohesin binding and transcription at the BDNF locus. Proc. Natl. Acad. Sci. U.S.A. 107, 21836–21841. https://doi.org/10.1073/pnas.1002130107.

Chiarugi, A., Dölle, C., Felici, R., Ziegler, M., 2012. The NAD metabolome–a key determinant of cancer cell biology. Nat. Rev. Cancer 12, 741–752. https://doi.org/10.1038/nrc3340.

Chuang, J.-H., Tung, L.-C., Lin, Y., 2015. Neural differentiation from embryonic stem cells in vitro: an overview of the signaling pathways. World J. Stem Cell. 7, 437–447. https://doi.org/10.4252/wjsc.v7.i2.437.

da Rocha, J.F., Bastos, L., Domingues, S.C., Bento, A.R., Konietzko, U., da Cruz e Silva, O. A.B., Vieira, S.I., 2021. APP binds to the EGFR ligands HB-EGF and EGF, acting synergistically with EGF to promote ERK signaling and neuritogenesis. Mol. Neurobiol. 58, 668–688. https://doi.org/10.1007/s12035-020-02139-2.

da Rocha, J.F., da Cruz e Silva, O.A.B., Vieira, S.I., 2015. Analysis of the amyloid precursor protein role in neuritogenesis reveals a biphasic SH-SY5Y neuronal cell differentiation model. J. Neurochem. 134, 288–301. https://doi.org/10.1111/jnc.13133.

Dias, R.A., Gonçalves, B.P., da Rocha, J.F., da Cruz E Silva, O.A.B., da Silva, A.M.F., Vieira, S.I., 2017. NeuronRead, an open source semi-automated tool for morphometric analysis of phase contrast and fluorescence neuronal images. Mol. Cell. Neurosci. 85, 57–69. https://doi.org/10.1016/j.mcn.2017.08.002.

Diez, H., Garrido, J.J., Wandosell, F., 2012. Specific roles of Akt iso forms in apoptosis and axon growth regulation in neurons. PLoS One 7. https://doi.org/10.1371/journal.pone.0032715 e32715–e32715.

Duarte-Pereira, S., Fajarda, O., Matos, S., Luís Oliveira, J., Silva, R.M., 2021. NAPRT expression regulation mechanisms: novel functions predicted by a bioinformatics approach. Genes 12. https://doi.org/10.3390/genes12122022.

Duarte-Pereira, S., Pereira-Castro, I., Silva, S.S., Correia, M.G., Neto, C., da Costa, L.T., Amorim, A., Silva, R.M., 2016. Extensive regulation of nicotinate phosphoribosyltransferase (NAPRT) expression in human tissues and tumors. Oncotarget 7, 1973–1983.

Dwane, S., Durack, E., Kiely, P.A., 2013. Optimising parameters for the differentiation of SH-SY5Y cells to study cell adhesion and cell migration. BMC Res. Notes 6, 366. https://doi.org/10.1186/1756-0500-6-366.

Encinas, M., Iglesias, M., Liu, Y., Wang, H., Muhaisen, A., Ceña, V., Gallego, C., Comella, J.X., 2000. Sequential treatment of SH-SY5Y cells with retinoic acid and brain-derived neurotrophic factor gives rise to fully differentiated, neurotrophic factor-dependent, human neuron-like cells. J. Neurochem. 75, 991–1003. https://doi.org/10.1046/j.1471-4159.2000.0750991.x.

Fletcher, R.S., Ratajczak, J., Doig, C.L., Oakey, L.A., Callingham, R., Da Silva Xavier, G., Garten, A., Elhassan, Y.S., Redpath, P., Migaud, M.E., Philp, A., Brenner, C., Canto, C., Lavery, G.G., 2017. Nicotinamide riboside kinases display redundancy in mediating nicotinamide mononucleotide and nicotinamide riboside metabolism in skeletal muscle cells. Mol. Metabol. 6, 819–832. https://doi.org/10.1016/j.molmet.2017.05.011.

Fu, J., Zhang, H., Zhang, Y., Zhang, T., 2019. AG1031 induces apoptosis through suppressing SIRT1/p53 pathway in human neuroblastoma cells. Mol. Cell. Biochem. 454, 165–175. https://doi.org/10.1007/s11010-018-3461-2.

Fulco, M., Schiltz, R.L., Iezzi, S., King, M.T., Zhao, P., Kashiwaya, Y., Hoffman, E., Veech, R.L., Sartorelli, V., 2003. Sir2 regulates skeletal muscle differentiation as a potential sensor of the redox state. Mol. Cell. 12, 51–62. https://doi.org/10.1016/S1097-2765(03)00226-0.

Galli, U., Colombo, G., Travelli, C., Tron, G.C., Genazzani, A.A., Grolla, A.A., 2020. Recent advances in NAMPT inhibitors: a novel immunotherapic strategy. Front. Pharmacol. 11, 656. https://doi.org/10.3389/fphar.2020.00656.

Gaub, P., Tedeschi, A., Puttagunta, R., Nguyen, T., Schmandke, A., Di Giovanni, S., 2010. HDAC inhibition promotes neuronal outgrowth and counteracts growth cone collapse through CBP/p300 and P/CAF-dependent p53 acetylation. Cell Death Differ. 17, 1392–1408. https://doi.org/10.1038/cdd.2009.216.

Guo, L., Lin, W., Zhang, Y., Wang, J., 2020. A systematic analysis revealed the potential gene regulatory processes of ATRA-triggered neuroblastoma differentiation and identified a novel RA response sequence in the NTRK2 gene. BioMed Res. Int. 2020, 6734048 https://doi.org/10.1155/2020/6734048.

Hara, N., Yamada, K., Shibata, T., Osago, H., Hashimoto, T., Tsuchiya, M., 2007. Elevation of cellular NAD levels by nicotinic acid and involvement of nicotinic acid phosphoribosyltransferase in human cells. J. Biol. Chem. 282, 24574–24582. https://doi.org/10.1074/jbc.M610357200.

Haslinger, D., Waltes, R., Yousaf, A., Lindlar, S., Schneider, I., Lim, C.K., Tsai, M.-M., Garvalov, B.K., Acker-Palmer, A., Krezdorn, N., Rotter, B., Acker, T., Guillemin, G.J., Fulda, S., Freitag, C.M., Chiocchetti, A.G., 2018. Loss of the Chr16p11.2 ASD candidate gene QPRT leads to aberrant neuronal differentiation in the SH-SY5Y neuronal cell model. Mol. Autism. 9, 56. https://doi.org/10.1186/s13229-018-0239-z.

He, X., He, J., Shi, Y., Pi, C., Yang, Y., Sun, Y., Ma, C., Lin, L., Zhang, L., Li, Yulin, Li, Yan, 2017. Nicotinamide phosphoribosyltransferase (Nampt) may serve as the marker for osteoblast differentiation of bone marrow-derived mesenchymal stem cells. Exp. Cell Res. 352, 45–52. https://doi.org/10.1016/j.yexcr.2017.01.021.

Hernandez-Martinez, J.-M., Forrest, C.M., Darlington, L.G., Smith, R.A., Stone, T.W., 2017. Quinolinic acid induces neuritogenesis in SH-SY5Y neuroblastoma cells independently of NMDA receptor activation. Eur. J. Neurosci. 45, 700–711. https://doi.org/10.1111/ejn.13499.

Hisahara, S., Chiba, S., Matsumoto, H., Tanno, M., Yagi, H., Shimohama, S., Sato, M., Horio, Y., 2008. Histone deacetylase SIRT1 modulates neuronal differentiation by its nuclear translocation. Proc. Natl. Acad. Sci. USA 105, 15599. https://doi.org/10.1073/pnas.0800612105. LP – 15604.

Huang, Q., Zhou, D., Sapp, E., Aizawa, H., Ge, P., Bird, E.D., Vonsattel, J.P., DiFiglia, M., 1995. Quinolinic acid-induced increases in calbindin D28k immunoreactivity in rat striatal neurons in vivo and in vitro mimic the pattern seen in Huntington's disease. Neuroscience 65, 397–407. https://doi.org/10.1016/0306-4522(94)00494-p.

Huang, X., Guo, H., Cheng, X., Zhang, J., Qu, W., Ding, Q., Sun, Q., Shu, Q., Li, X., 2022. NAD+ modulates the proliferation and differentiation of adult neural stem/progenitor cells via akt signaling pathway. Cells 11. https://doi.org/10.3390/cells11081283.

Imai, S., Guarente, L., 2014. NAD+ and sirtuins in aging and disease. Trends Cell Biol. 24, 464–471. https://doi.org/10.1016/j.tcb.2014.04.002.

Kim, B.S., Lee, C.-H., Chang, G.-E., Cheong, E., Shin, I., 2016. A potent and selective small molecule inhibitor of sirtuin 1 promotes differentiation of pluripotent P19 cells into functional neurons. Sci. Rep. 6, 34324 https://doi.org/10.1038/srep34324.

Lee, J., Kim, Hyosil, Lee, J.E., Shin, S.-J., Oh, S., Kwon, G., Kim, Hakhyun, Choi, Y.Y., White, M.A., Paik, S., Cheong, J.-H., Kim, H.S., 2018. Selective cytotoxicity of the NAMPT inhibitor FK866 toward gastric cancer cells with markers of the epithelial-mesenchymal transition. Due to Loss of NAPRT. Gastroenterology 155, 799–814. https://doi.org/10.1053/j.gastro.2018.05.024 e13.

Li, X.-H., Chen, C., Tu, Y., Sun, H.-T., Zhao, M.-L., Cheng, S.-X., Qu, Y., Zhang, S., 2013. Sirt1 promotes axonogenesis by deacetylation of Akt and inactivation of GSK3. Mol. Neurobiol. 48, 490–499. https://doi.org/10.1007/s12035-013-8437-3.

Lugo-Huitrón, R., Ugalde Muñiz, P., Pineda, B., Pedraza-Chaverrí, J., Ríos, C., Pérez-de la Cruz, V., 2013. Quinolinic acid: an endogenous neurotoxin with multiple targets. Oxid. Med. Cell. Longev., 104024 https://doi.org/10.1155/2013/104024, 2013.

Managò, A., Audrito, V., Mazzola, F., Sorci, L., Gaudino, F., Gizzi, K., Vitale, N., Incarnato, D., Minazzato, G., Ianniello, A., Varriale, A., D'Auria, S., Mengozzi, G., Politano, G., Oliviero, S., Raffaelli, N., Deaglio, S., 2019. Extracellular nicotinate phosphoribosyltransferase binds Toll like receptor 4 and mediates inflammation. Nat. Commun. 10, 4116. https://doi.org/10.1038/s41467-019-12055-2.

Matsuno, H., Tsuchimine, S., Fukuzato, N., O'Hashi, K., Kunugi, H., Sohya, K., 2021. Sirtuin 6 is a regulator of dendrite morphogenesis in rat hippocampal neurons. Neurochem. Int. 145, 104959 https://doi.org/10.1016/j.neuint.2021.104959.

Meng, Y., Ren, Z., Xu, F., Zhou, X., Song, C., Wang, V.Y.-F., Liu, W., Lu, L., Thomson, J.A., Chen, G., 2018. Nicotinamide promotes cell survival and differentiation as kinase inhibitor in human pluripotent stem cells. Stem Cell Rep. 11, 1347–1356. https://doi.org/10.1016/j.stemcr.2018.10.023.

Ozden, O., Park, S.-H., Wagner, B.A., Yong Song, H., Zhu, Y., Vassilopoulos, A., Jung, B., Buettner, G.R., Gius, D., 2014. SIRT3 deacetylates and increases pyruvate dehydrogenase activity in cancer cells. Free Radic. Biol. Med. 76, 163–172. https://doi.org/10.1016/j.freeradbiomed.2014.08.001.

Piacente, F., Caffa, I., Ravera, S., Sociali, G., Passalacqua, M., Vellone, V.G., Becherini, P., Reverberi, D., Monacelli, F., Ballestrero, A., Odetti, P., Cagnetta, A., Cea, M., Nahimana, A., Duchosal, M., Bruzzone, S., Nencioni, A., 2017. Nicotinic acid phosphoribosyltransferase regulates cancer cell metabolism, susceptibility to NAMPT inhibitors, and DNA repair. Cancer Res. 77, 3857. https://doi.org/10.1158/0008-5472.CAN-16-3079. LP – 3869.

Prozorovski, T., Schulze-Topphoff, U., Glumm, R., Baumgart, J., Schröter, F., Ninnemann, O., Siegert, E., Bendix, I., Brüstle, O., Nitsch, R., Zipp, F., Aktas, O., 2008. Sirt1 contributes critically to the redox-dependent fate of neural progenitors. Nat. Cell Biol. 10, 385–394. https://doi.org/10.1038/ncb1700.

Rajman, L., Chwalek, K., Sinclair, D.A., 2018. Therapeutic potential of NAD-boosting molecules: the in vivo evidence. Cell Metabol. 27, 529–547. https://doi.org/10.1016/j.cmet.2018.02.011.

Ryu, K.W., Nandu, T., Kim, J., Challa, S., DeBerardinis, R.J., Lee Kraus, W., 2018. Metabolic regulation of transcription through compartmentalized NAD+ biosynthesis. Science 80, 360. https://doi.org/10.1126/science.aan5780.

Şahin, M., Öncü, G., Yılmaz, M.A., Özkan, D., Saybaşılı, H., 2021. Transformation of SH-SY5Y cell line into neuron-like cells: investigation of electrophysiological and biomechanical changes. Neurosci. Lett. 745, 135628 https://doi.org/10.1016/j.neulet.2021.135628.

Shannon, P., Markiel, A., Ozier, O., Baliga, N.S., Wang, J.T., Ramage, D., Amin, N., Schwikowski, B., Ideker, T., 2003. Cytoscape: a software environment for integrated models of biomolecular interaction networks. Genome Res. 13, 2498–2504. https://doi.org/10.1101/gr.1239303.

Shukla, S., Tekwani, B.L., 2020. Histone deacetylases inhibitors in neurodegenerative diseases, neuroprotection and neuronal differentiation. Front. Pharmacol. 11, 537. https://doi.org/10.3389/fphar.2020.00537.

Sierra-Fonseca, J.A., Najera, O., Martinez-Jurado, J., Walker, E.M., Varela-Ramirez, A., Khan, A.M., Miranda, M., Lamango, N.S., Roychowdhury, S., 2014. Nerve growth factor induces neurite outgrowth of PC12 cells by promoting Gβγ-microtubule interaction. BMC Neurosci. 15, 132. https://doi.org/10.1186/s12868-014-0132-4.

Skokowa, J., Lan, D., Thakur, B.K., Wang, F., Gupta, K., Cario, G., Brechlin, A.M., Schambach, A., Hinrichsen, L., Meyer, G., Gaestel, M., Stanulla, M., Tong, Q., Welte, K., 2009. NAMPT is essential for the G-CSF-induced myeloid differentiation via a NAD(+)-sirtuin-1-dependent pathway. Nat. Med. 15, 151–158. https://doi.org/10.1038/nm.1913.

Stein, L.R., Imai, S., 2014. Specific ablation of Nampt in adult neural stem cells recapitulates their functional defects during aging. EMBO J. 33, 1321–1340. https://doi.org/10.1002/embj.201386917.

Tang, S., Huang, G., Fan, W., Chen, Y., Ward, J.M., Xu, X., Xu, Q., Kang, A., McBurney, M.W., Fargo, D.C., Hu, G., Baumgart-Vogt, E., Zhao, Y., Li, X., 2014. SIRT1-Mediated deacetylation of CRABPII regulates cellular retinoic acid signaling and modulates embryonic stem cell differentiation. Mol. Cell. 55, 843–855. https://doi.org/10.1016/j.molcel.2014.07.011.

Tojima, T., Kobayashi, S., Ito, E., 2003. Dual role of cyclic AMP-dependent protein kinase in neuritogenesis and synaptogenesis during neuronal differentiation. J. Neurosci. Res. 74, 829–837. https://doi.org/10.1002/jnr.10754.

Varderidou-Minasian, S., Verheijen, B.M., Schätzle, P., Hoogenraad, C.C., Pasterkamp, R. J., Altelaar, M., 2020. Deciphering the proteome dynamics during development of neurons derived from induced pluripotent stem cells. J. Proteome Res. 19, 2391–2403. https://doi.org/10.1021/acs.jproteome.0c00070.

Vojtek, A.B., Taylor, J., DeRuiter, S.L., Yu, J.-Y., Figueroa, C., Kwok, R.P.S., Turner, D.L., 2003. Akt regulates basic helix-loop-helix transcription factor-coactivator complex formation and activity during neuronal differentiation. Mol. Cell Biol. 23, 4417–4427. https://doi.org/10.1128/MCB.23.13.4417-4427.2003.

Xu, Y., Nasri, M., Dannenmann, B., Mir, P., Zahabi, A., Welte, K., Morishima, T., Skokowa, J., 2021. NAMPT/SIRT2-mediated inhibition of the p53-p21 signaling pathway is indispensable for maintenance and hematopoietic differentiation of human iPS cells. Stem Cell Res. Ther. 12, 112. https://doi.org/10.1186/s13287-021-02144-9.

Yap, C.C., Winckler, B., 2012. Harnessing the power of the endosome to regulate neural development. Neuron 74, 440–451. https://doi.org/10.1016/j.neuron.2012.04.015.

Yu, S., Levi, L., Siegel, R., Noy, N., 2012. Retinoic acid induces neurogenesis by activating both retinoic acid receptors (RARs) and peroxisome proliferator-activated receptor β/δ (PPARβ/δ). J. Biol. Chem. 287, 42195–42205. https://doi.org/10.1074/jbc.M112.410381.

Zhang, T., Gygi, S.P., Paulo, J.A., 2021. Temporal proteomic profiling of SH-SY5Y differentiation with retinoic acid using FAIMS and real-time searching. J. Proteome Res. 20, 704–714. https://doi.org/10.1021/acs.jproteome.0c00614.

Zocchi, L., Sassone-Corsi, P., 2012. SIRT1-mediated deacetylation of MeCP2 contributes to BDNF expression. Epigenetics 7, 695–700. https://doi.org/10.4161/epi.20733.